Received: 31 January 2019 | Revised: 22 May 2019 | Accepted: 22 May 2019

DOI: 10.1111/epi.16073

FULL-LENGTH ORIGINAL RESEARCH

Epilepsia®

Sulfasalazine decreases mouse cortical hyperexcitability

Oscar Alcoreza[1] | Bhanu P. Tewari[2] | Allison Bouslog[1] | Andrew Savoia[3] | Harald Sontheimer[2,3] | Susan L. Campbell[3,4]

[1]Fralin Biomedical Research Institute, Translational Biology, Medicine and Health, Virginia Tech, Roanoke, Virginia

[2]Fralin Biomedical Research Institute, Glial Biology in Health, Disease and Cancer, Virginia Tech, Roanoke, Virginia

[3]School of Neuroscience, Virginia Tech, Blacksburg, Virginia

[4]Animal and Poultry Sciences, Virginia Tech, Blacksburg, Virginia

Correspondence
Susan L. Campbell Animal and Poultry Sciences, 2200 Litton Reaves Hall, Virginia Tech, Blacksburg, 24061 VA.
Email: susanc08@vt.edu

Funding information
Foundation for the National Institutes of Health, Grant/Award Number: 5R01-NS036692, R01-NS052634 and R01CA227149

Abstract

Objective: Currently prescribed antiepileptic drugs (AEDs) are ineffective in treating approximately 30% of epilepsy patients. Sulfasalazine (SAS) is an US Food and Drug Administration (FDA)–approved drug for the treatment of Crohn disease that has been shown to inhibit the cystine/glutamate antiporter system xc- (SXC) and decrease tumor-associated seizures. This study evaluates the effect of SAS on distinct pharmacologically induced network excitability and determines whether it can further decrease hyperexcitability when administered with currently prescribed AEDs.

Methods: Using in vitro cortical mouse brain slices, whole-cell patch-clamp recordings were made from layer 2/3 pyramidal neurons. Epileptiform activity was induced with bicuculline (bic), 4-aminopyridine (4-AP) and magnesium-free (Mg^{2+}-free) solution to determine the effect of SAS on epileptiform events. In addition, voltage-sensitive dye (VSD) recordings were performed to characterize the effect of SAS on the spatiotemporal spread of hyperexcitable network activity and compared to currently prescribed AEDs.

Results: SAS decreased evoked excitatory postsynaptic currents (eEPSCs) and increased the decay kinetics of evoked inhibitory postsynaptic currents (eIPSCs) in layer 2/3 pyramidal neurons. Although application of SAS to bic and Mg^{2+}-free–induced epileptiform activity caused a decrease in the duration of epileptiform events, SAS completely blocked 4-AP–induced epileptiform events. In VSD recordings, SAS decreased VSD optical signals induced by 4-AP. Co-application of SAS with the AED topiramate (TPM) caused a significantly further decrease in the spatiotemporal spread of VSD optical signals.

Significance: Taken together this study provides evidence that inhibition of SXC by SAS can decrease network hyperexcitability induced by three distinct pharmacologic agents in the superficial layers of the cortex. Furthermore, SAS provided additional suppression of 4-AP–induced network activity when administered with the currently prescribed AED TPM. These findings may serve as a foundation to assess

Oscar Alcoreza and Bhanu P. Tewari contributed equally.

the potential for SAS or other compounds that selectively target SXC as an adjuvant treatment for epilepsy.

KEYWORDS
antiepileptic drugs, epilepsy, seizure, sulfasalazine, system xc-

1 | INTRODUCTION

Epilepsy is the most chronic and progressive neurologic disorder and affects an estimated 50 million individuals worldwide. One in 26 people will develop epilepsy within their lifetime.[1] Despite the development of numerous antiepileptic drugs (AEDs) over the past 20 years, which provide more options for clinicians and patients, current treatment regimens fail in up to 30% of patients.[2,3] This increase in treatment options has prompted an interest in the efficacy of combination AED therapy to utilize drugs with differing pharmacologic properties.

Because most AEDs were generated by targeting neuronal inhibitory and excitatory mechanisms, the contribution of glial cells to the pathophysiology of epilepsy is increasingly being explored.[4] In addition, it is widely accepted that astrocyte dysfunction is a crucial player in epilepsy[5,6] One potential new target is SXC, a glutamate/cystine antiporter primarily expressed on astrocytes, which has been implicated in several psychological and neurologic disorders.[7] SXC knockout mice were found to be less susceptible to seizure induction compared to wild types, and the increased threshold was attributed to a 40% reduction in extracellular hippocampal glutamate levels.[8] In addition to its role in glutamatergic signaling, SXC plays a major role in the cystine/cysteine cycle. SXC mediates the uptake of cystine into astrocytes, which is then reduced to cysteine and released to be taken up by neurons as the rate-limiting precursor for the synthesis of glutathione, a critical antioxidant.[9] The role of SXC, at the crossroads between excitatory signaling and managing oxidative stress, makes it an intriguing target for the treatment and prevention of acquired epilepsy.

Sulfasalazine (SAS) is a US Food and Drug Administration (FDA)–approved drug for rheumatoid arthritis and inflammatory bowel disease. We previously showed that SAS decreased tumor-associated seizures in a mouse model of glioma.[10] In this model, glutamate release by glioblastoma cells, via SXC, induced peritumoral neuronal excitotoxicity and contributed to tumor-associated epilepsy. A subsequent pilot clinical study found that acute SAS treatment reduced extracellular glutamate levels by inhibiting SXC in patients with glioma.[11]

Because the mechanisms of seizure development involve a complex interplay of aberrant neuronal network activity,[12] various in vitro pharmacologic models of hyperexcitability have been utilized to assess novel AEDs. Use of Mg^{2+}-free artificial cerebrospinal fluid (ACSF) for in vitro electrophysiology removes the magnesium block from *N*-methyl-D-aspartate (NMDA) receptors, resulting in neuronal hyperexcitability, as described previously.[13] As a γ-aminobutyric acid receptor A ($GABA_A$) antagonist, bicuculline (bic) simulates neuronal hyperexcitability by decreasing inhibition, whereas 4-aminopyridine (4-AP) reduces neuronal K^+ repolarization. Although all chemically induced models are valuable for studying seizure mechanisms, variations in models can affect end results.

In this study, we used whole-cell patch-clamp recordings of layer II/III pyramidal cells and voltage-sensitive dye (VSD) imaging to evaluate the effect of SAS on three chemically induced in vitro models of hyperexcitability. Our findings indicate that SAS has significant effects on decreasing hyperexcitability at the cellular and network levels in all the pharmacologically induced models we tested. In addition, we provide evidence that concomitant use of topiramate (TPM), an AED used to treat generalized-onset tonic-clonic seizures,[14] and SAS results in additional antiepileptic effects, compared to the use of TPM alone. Based on these findings, we believe that further investigation of SXC and its modulation by SAS may allow us to unravel some of the complex, extrasynaptic processes associated with the pathogenesis of

Key Points

- The present study describes the effect of SXC on eEPSCs, eIPSCs, and three pharmacologically induced hyperexcitability models in cortical mouse slices
- SAS decrease eEPSC amplitude and prolonged eIPSC decay time
- SAS attenuated bic and Mg^{2+}-free–induced cortical network hyperexcitability and completely blocked 4-AP–induced hyperexcitability
- SAS was more efficacious in decreasing the spread and duration of 4-AP–induced VSD optical response compared to the currently prescribed AED TPM
- SXC could be considered as an additional therapeutic target for the treatment of epilepsy

acquired epilepsy, which could lead to novel therapeutics for patients with intractable epilepsy.

2 | MATERIALS AND METHODS

2.1 | Animals

Animals were housed and handled according to the guidelines of the National Institutes of Health Committee on Laboratory Animal Resources. Prior approval of the University of Alabama at Birmingham Institutional Animal Care and Use Committee was obtained for all experimental protocols. All efforts were made to minimize pain. Experiments were performed using 4- to 6-week-old C57Bl6 mice.

2.2 | Slice preparation

Mice were anesthetized and decapitated and their brains were quickly removed and immersed in ice-cold cutting solution containing (in mmol/L): 135 *N*-methyl-D-glucamine (NMDG), 1.5 KCl, 1.5 KH_2PO_4, 23 mmol/L choline bicarbonate, 25 D-glucose, 0.5 mmol/L $CaCl_2$, and 3.5 $MgSO_4$ (Sigma-Aldrich). Coronal brain slices (300 μm) were made and recovered for 40-60 minutes in oxygenated recording solution in mmol/L: 125 NaCl, 3 KCl, 1.25 NaH_2PO_4, 25 $NaHCO_3$, 2 CaCl2, 1.3 $MgSO_4$, and 25 D-glucose at 32°C and maintained at room temperature before recordings.

2.3 | Whole-cell recordings

Individual brain slices were transferred to a recording chamber and continuously perfused (4 mL/min) with oxygenated recording solution. Whole-cell recordings were conducted using borosilicate glass capillaries (KG-33 glass, Garner Glass) and filled with internal solution containing (in mmol/L): 134 K-gluconate, 1 KCl, 10 HEPES, 2 mg-ATP; 0.2 Na-GTP and 0.5 ethylene glycol tetraacetic acid (EGTA). The pH was set to 7.24 with KOH, and the osmolality was measured (~290 mOsm/kg). All recordings were performed at 32 ± 1°C. Individual cells were visualized using a Zeiss Axioscope (Carl Zeiss) microscope equipped with Nomarski optics with a 40× water-immersion objective lens. Tight seals were made using electrodes with a 3–5-MΩ open-tip resistance. Signals were acquired from layer II/III pyramidal cells with an Axopatch 1B amplifier (Molecular Devices), controlled by Clampex 10 software via a Digidata 1440 interface (Molecular Devices). To isolate GABAergic inhibitory postsynaptic currents (IPSCs), slices were perfused with ACSF containing 20 μmol/L 6-cyano-7-nitroquinoxaline-2,3-dione (CNQX, Fisher), and 50 μmol/L D-(-)-2-amino-5-phosphonovaleric acid (APV, Sigma) and recorded at −70 mV. Excitatory postsynaptic currents (EPSCs) were obtained in the presence of bic (10 μmol/L; Sigma-Aldrich) to block $GABA_A$ receptors. *N*-methyl-D-aspartate (NMDA) receptor–mediated currents were isolated in the presence of bic and CNQX and recorded at −40 mV. AMPA receptor–mediated EPSCs were isolated at a holding potential of −70 mV in the presence of bic and APV. A twisted pair of Formvar-insulated nichrome wires was positioned in deeper cortical layer IV to evoke synaptic responses. Stimulation intensity was 20 −200 μA pulses for 50 μs at 0.05 Hz. Representative traces are averages of 10 consecutive responses. Responses were filtered at 5 kHz, digitized at 10-20 kHz, and analyzed off-line with Clampfit 10.0 software.

2.4 | Voltage-sensitive dye imaging

Optical recordings were conducted using the voltage-sensitive fluorescent dye N-[3-(triethylammonium)propyl]-4-[4-(p-diethylaminophenyl)butadienyl]pyridinium dibromide (RH 414). Individual slices were incubated with 30 μmol/L RH414 for at least 60 minutes, and then slices were transferred to a recording chamber on an Axiovert 135 TV (Zeiss) microscope. The microscope was equipped with NeuroPlex 464-element photodiode array (Red Shirt Imaging), as described previously.[15] A bipolar stimulating electrode placed in cortical layer IV was used to evoke activity, with stimulation intensities from 20 to 100 μA in amplitude and 100 μs in duration. Changes in fluorescence were detected by a hexagonal photodiode array containing 464 diodes (NeuroPlex, Red Shirt Imaging). Excitation of the dye was achieved with a stabilized power supply (Hewlett-Packard), a 100-W halogen lamp, and a 535 ± 40 nm filter. Fluorescent measurements were obtained by normalizing the resting light intensity for each diode. Dye bleaching corrections were done by acquiring measurements in the absence of stimulation. Optical signals are represented as change in fluorescence with stimulation divided by resting fluorescence (ΔF/F). The responses to three consecutive stimulations were averaged. RH 414 responds to membrane depolarization with a decrease in the fluorescence intensity. Optical signals were amplified and stored on a computer for later analysis. Pseudocolor images were generated to visualize spatiotemporal spread of activity.

2.5 | Drug application

All drugs were bath applied. SAS (Fisher) was dissolved in 0.1N NaOH solution to create a 10 mmol/L stock solution and used at 250 μmol/L. 4-AP (50 μmol/L), TPM (50 μmol/L), and levetiracetam (LEV) (100 μmol/L) were purchased from Sigma-Aldrich. S-4CPG (100 μmol/L) was purchased from Tocris. For VSD recordings, slices were

exposed to bic (10 μmol/L), 4-AP, and Mg^{2+}-free for at least 45 minutes before recordings. TPM, LEV, and SAS were incubated for 30 minutes before recordings. In co-application experiments, SAS was added in the presence of LEV and TPM.

2.6 | Statistics

Changes in evoked E/IPSCs were analyzed using Clampfit Software 10.0 (Molecular Devices). Paired Student's *t* test was used for means comparisons among the number and

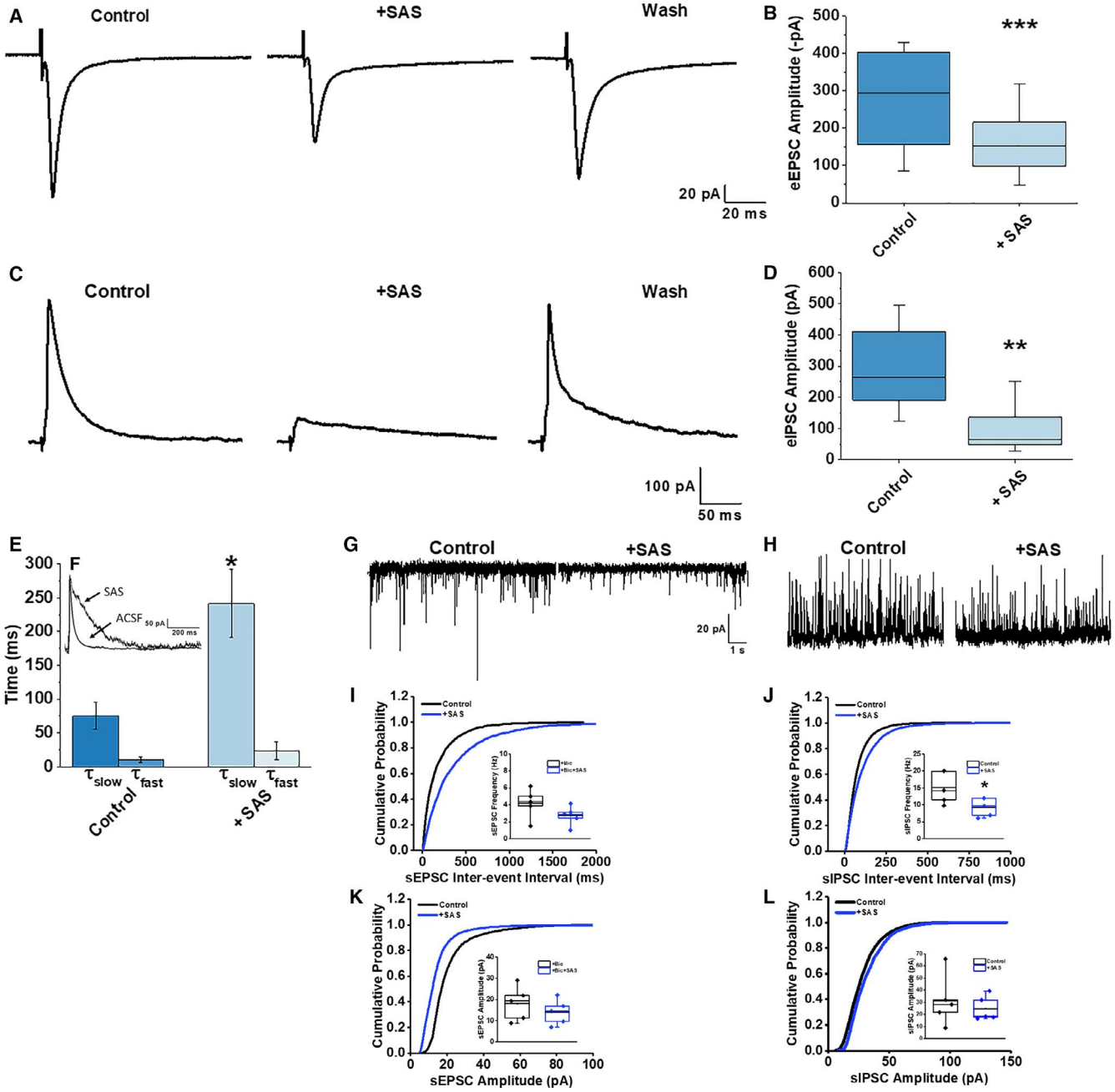

FIGURE 1 SAS decreases synaptic responses in layer II/III pyramidal cells. A, Representative traces of eEPSCs of a layer II/III pyramidal cell in an acute cortical slice before (left), during a 10-min application of SAS (middle), and after a wash (right). B, Quantitative summary of the eEPSC amplitude before and in the presence of SAS. *** = significantly different than control, n = 9, $P = 0.001$. C, Representative traces eIPSCs of layer II/III pyramidal cells in an acute cortical slice before (left), during a 10-min application of SAS (middle), and after a wash (right). D, Quantitative summary of the eIPSC amplitude. ** = significantly different than control, n = 6, $P = 0.003$. E, Quantitative summary of τ_{slow} and τ_{fast} eIPSC decay kinetics before and in the presence of SAS. * = τ_{slow} + SAS is significantly different from τ_{slow} Control, n = 6, $P = 0.03$. (F, inset) Normalized eIPSC traces from control (ACSF) and SAS-treated slices. Representative traces of sEPSCs (G) and spontaneous inhibitory postsynaptic currents (sIPSCs) (H) of layer II/III pyramidal cells in an acute slice before (left) and during SAS application (right). I, Cumulative probability plot and average values (inset) of sEPSC frequency and amplitude (J). K, Cumulative probability plot and average values (inset) of sIPSC frequency and amplitude (L)

duration of epileptiform events, and amplitude of currents in whole-cell recordings. A two-way repeated-measures analysis of variance (ANOVA; varying conditions as between-subject factors and stimulation intensity as a repeated measure) and Tukey's post hoc tests were used for statistical comparison of VSD recordings. Statistics were generated and graphed using Origin 7.5 Pro software (Origin), with significance set at $P < 0.05$. Figures display box-and-whisker plots (minimum to maximum, median line) or histograms (mean ± standard error of mean). Values in the text report mean ± standard deviation.

3 | RESULTS

3.1 | Sulfasalazine decreases evoked excitatory postsynaptic currents (eEPSCs)

We first examined the effects of SAS on eEPSCs using whole-cell patch-clamp recordings of layer II/III pyramidal cells in the prefrontal cortex. Synaptic responses were elicited via intracortical stimulations 150-200 μm below the recording pipette. We isolated eEPSCs by recording in the presence of bic to block $GABA_A$ receptor–mediated currents and cells were held at −70 mV. Following baseline recordings, infusion of

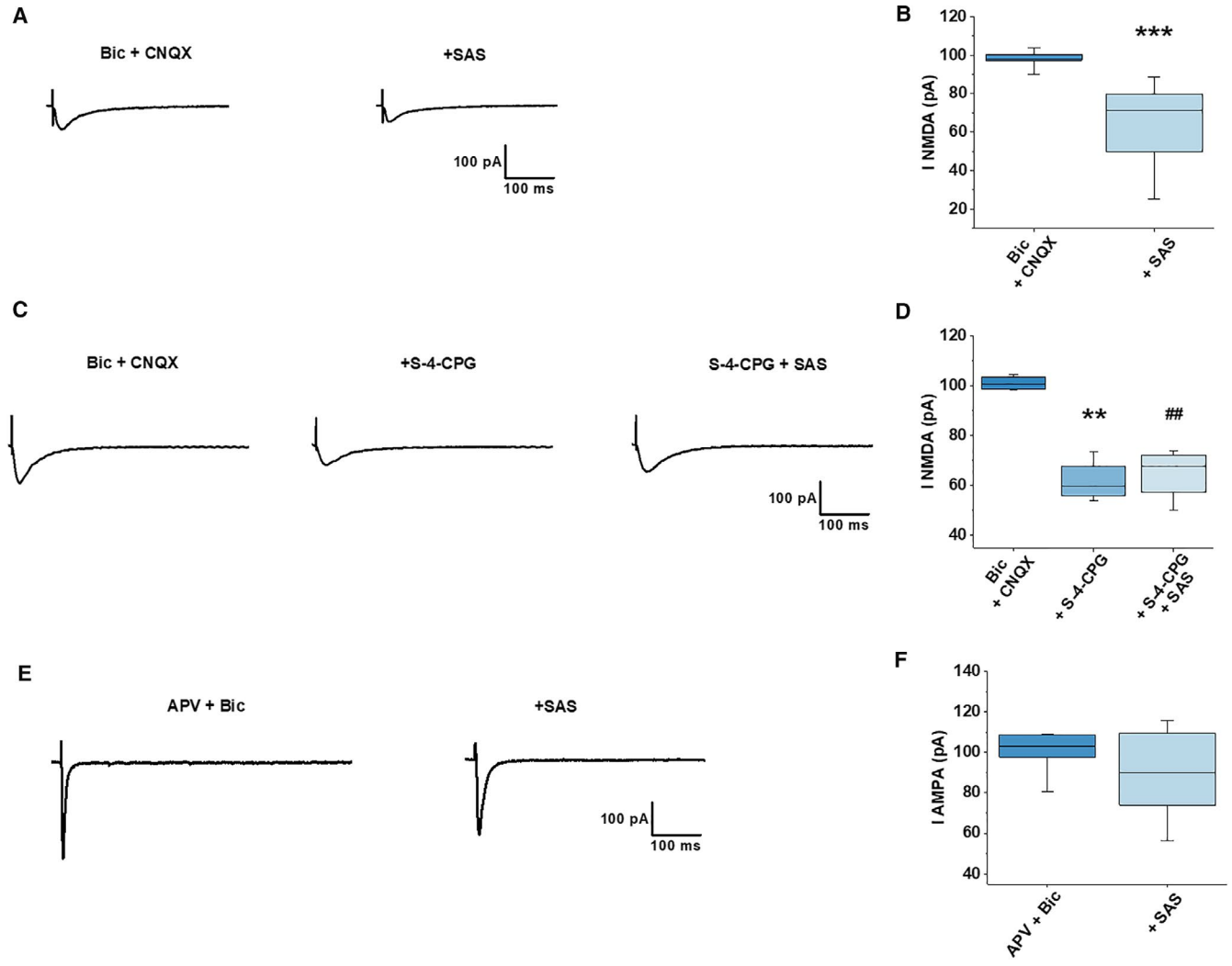

FIGURE 2 SAS decreases NMDAR-mediated currents. A, Representative traces of isolated NMDAR-mediated currents before (left) and after application of SAS (right). B, Quantitative summary of isolated NMDA EPSCs before and after SAS application. *** = SAS application significantly different than bic + CNQX, n = 13, $P < 0.001$. C, Representative traces of isolated NMDAR-mediated currents (left), in the presence of S-4-CPG (middle), and during co-application of SAS (right). D, Quantitative summary of isolated NMDA EPSCs under control conditions, in the presence of S-4-CPG, and with co-application of S-4-CPG + SAS. ** = S-4-CPG application significantly different than bic + CNQX, n = 4, $P = 0.004$. # = S-4-CPG + SAS co-application significantly different than bic + CNQX, n = 4, $P = 0.01$. E, Representative traces of isolated AMPAR EPSCs (left) and response to SAS application (right). F, Time course experiment showing the effect of SAS on AMPA EPSCs amplitude. No significant change was detected (n = 8, $P = 0.23$)

SAS for 10 minutes reversibly decreased eEPSC amplitude (control: 289.43 ± 130.20 -pA; SAS: 172.41 ± 91.61 -pA, $P = 0.001$, Figure 1A,B).

3.2 | Sulfasalazine decreases evoked inhibitory postsynaptic currents (eIPSCs)

To investigate the effects of SAS on eIPSCs, we obtained whole-cell patch-clamp recordings in the presence of APV (20 μmol/L) and CNQX (10 μmol/L) to block ionotropic glutamate receptors. We found that bath application of SAS significantly decreased the eIPSC amplitude (control: 291.92 ± 139.82 pA; SAS: 98.40 ± 83.49 pA, $P = 0.003$, Figure 1C,D). When the current decay of eIPSC was fit by a sum of two exponentials, we observed a significant increase in the decay kinetics of the τ_{slow} response in the presence of SAS (control τ_{slow}: 75.31 ± 48.19 msec; SAS τ_{slow}: 241.30 ± 124.30 msec, $P = 0.03$, Figure 1E,F). The τ_{fast} response was not significantly altered by SAS (control τ_{fast}: 10.18 ± 9.84; SAS τ_{fast}: 23.96 ± 32.17 msec, $P = 0.42$, Figure 1E,F). These effects appeared to be reversible as eIPSC amplitude partially recovered during a 10-minute wash (Figure 1C, right). The prolongation of τ_{slow} did not significantly affect the response area (control, 7591 ± 1642 pA* msec; SAS, 9858 ± 3124 pA* msec, $P = 0.5$).

To understand if SAS alters basal synaptic transmission, we compared the frequency and amplitude of sEPSCs and sIPSCs before and after application of SAS. Statistical analyses show significantly smaller sEPSC amplitudes (control: 18 ± 3 pA; SAS: 14 ± 2 pA, $P = 0.02$, Figure 1G) and a decrease in the frequency (control: 4.1 ± 0.7 Hz; SAS: 2.7 ± 0.5 Hz, $P = 0.02$, Figure 1H). For sIPSCs, we found a significant decrease in the frequency (control: 15 ± 2 pA; SAS: 9 ± 1.2 pA, $P = 0.04$, Figure 1G) but no change in the amplitude (control: 31 ± 9 pA; SAS: 24 ± 5 pA, $P = 0.5$, Figure 1H) in response to SAS.

3.3 | Sulfasalazine decreases NMDAR-mediated currents

We wanted to test the effect of SAS on NMDA and AMPA receptor–mediated transmission during an evoked synaptic event. At a holding potential of −40 mV and in the presence of bic and CNQX, to block $GABA_A$- and AMPA receptor–mediated currents, respectively, the resulting NMDAR-mediated events were inward currents. Infusion of SAS resulted in a significant reduction in NMDA receptor–mediated currents (control: 97.93 ± 4.01 pA; SAS: 63.72 ± 21.01 pA, $P < 0.001$, Figure 2A,B). We also tested the effect of another SXC inhibitor, S-4-CPG (100 μmol/L), which resulted in a similar significant reduction in NMDA receptor–mediated current amplitude as SAS (control: 101.10 ± 2.82 pA; S-4-CPG: 61.74 ± 8.51 pA, $P = 0.004$, Figure 2C,D). Co-application of S-4-CPG and SAS did not result in further decrease of NMDA receptor–mediated current (S-4-CPG: 61.74 ± 8.51 pA; S-4-CPG+SAS: 64.74 ± 10.53 pA, $P = 0.69$, Figure 2C,D). To examine the effects of SAS on AMPA receptor–mediated currents, we recorded eEPSCs in the presence of bic and APV (Figure 2E, left), an NMDA-receptor antagonist. We did not observe a significant change in AMPA receptor–mediated eEPSCs (control: 101.16 ± 9.63 pA; SAS 89.98 ± 21.48 pA, $P = 0.23$, Figure 2E,F). These results indicate that SAS attenuates eEPSCs primarily via a reduction in NMDA receptor–mediated currents, supporting previous in vitro studies describing the NMDA antagonistic properties of SAS[16,17]

3.4 | Sulfasalazine decreases Mg^{2+}-free–induced cortical network hyperexcitability

The principal objective of this study was to determine whether inhibition of SXC, via SAS, can be explored as a novel therapeutic target for the treatment of acquired epilepsies. To this end, we used the SXC inhibitor SAS to question whether SAS could modulate epileptiform activity in distinct pharmacologically induced hyperexcitability models. Bath application of SAS reduced the amplitude of Mg^{2+}-free–induced epileptiform discharges but unveiled lower amplitudes and shorter interictal events (Figure 3A). Although the number of events did not significantly change with the addition of SAS (Mg^{2+}-free: 25.83 ± 16.58; SAS: 36.33 ± 26.34, $P = 0.48$, Figure 3B left), SAS significantly reduced the duration of the elicited events (Mg^{2+}-free: 4.13 ± 3.27 seconds; SAS: 0.55 ± 0.14 seconds, $P = 0.04$, Figure 3B right). Next, we assessed the effect of SAS on cortical network activity by using VSD recordings, which detects the spatiotemporal spread of neuronal network activity.[18,19] In the presence of the VSD RH-414, epileptiform network activity was elicited by intracortical stimulation in layer IV in cortical slices. Removal of Mg^{2+} from the recording solution causes an increase in the spread of VSD response. An example of Mg^{2+}-free–induced spatial dynamics of the VSD response is shown in Figure 3C (left). Each panel shows the spatial distribution and amplitude of dye signals at a given time point. Application of SAS for 30 minutes significantly decreased the peak amplitude (Figure 3C,D, $P < 0.001$) and the spread of the VSD signals (Figure 3C,D, $P < 0.001$) of Mg^{2+}-free–induced cortical network activity.

3.5 | Sulfasalazine decreases bic-induced epileptiform activity and completely blocked 4-AP–induced network hyperexcitability

Because SAS can act as a noncompetitive NMDA receptor antagonist [17] and the Mg^{2+}-free solution induces epileptiform activity by removing the Mg^{2+} block from NMDA receptors,

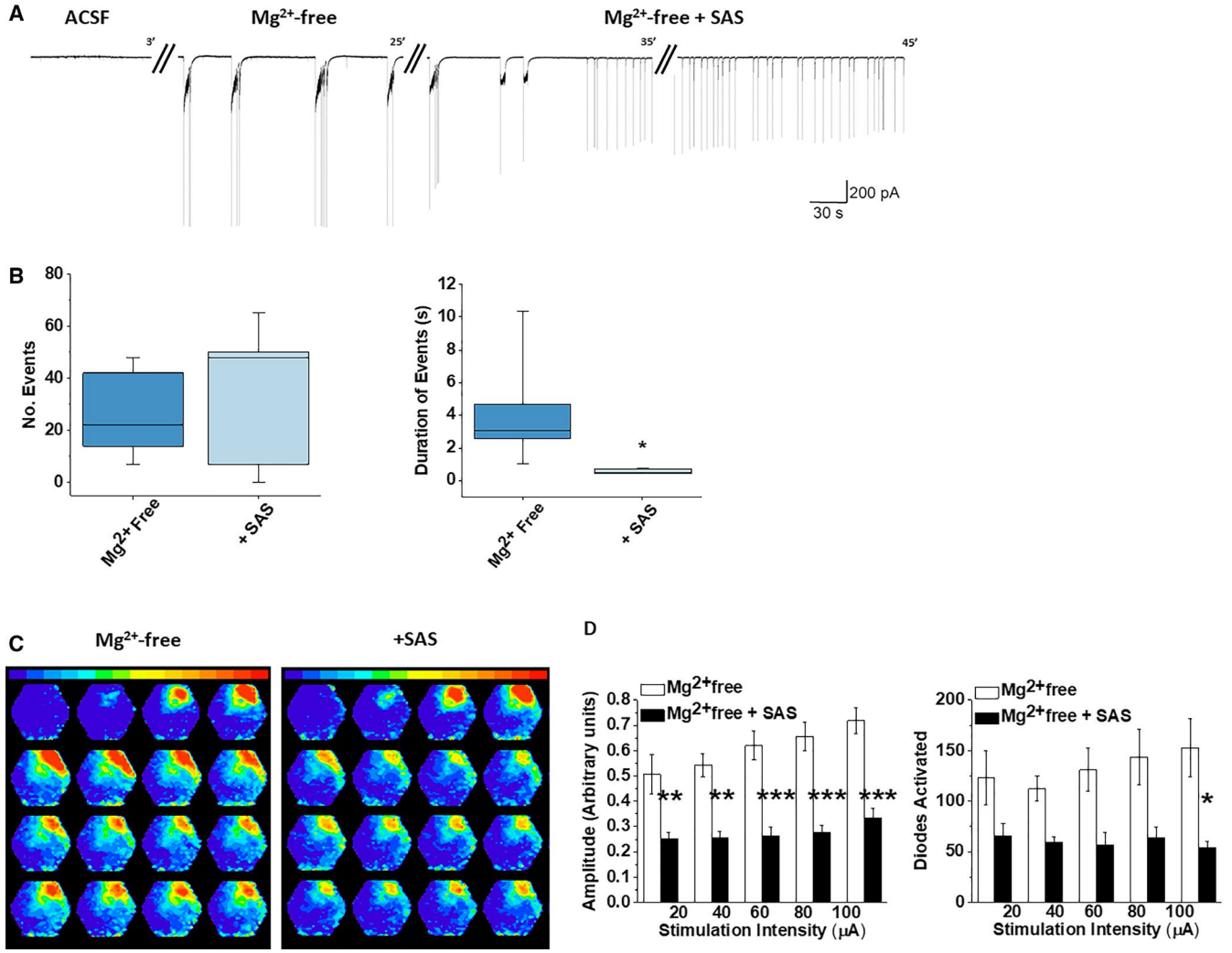

FIGURE 3 Effects of SAS on Mg^{2+}-free–induced epileptiform activity and VSD imaging network response. A, Representative traces of whole-cell patch clamp recordings depicting a decrease in Mg^{2+}-free–induced ictal events with SAS, but not interictal events. B, Quantitative summary of the number (left) (n = 6, $P = 0.48$) and duration (right) of epileptiform events detected in whole-cell patch clamp recordings. * = SAS application significantly different than Mg^{2+} -free, n = 6, $P = 0.04$. C, Representative optical recordings depicting the spatiotemporal spread of activity evoked in cortical slices in Mg^{2+}-free perfusate (left) and 30 min after the application of SAS (right). The pseudocolor images and dye signals depict a decrease in the large spread in VSD signal in the presence of SAS. D, Quantitative summary of the amplitude (left) and spread (right) of Mg^{2+}-free–induced VSD signals. SAS application significantly decreased the response amplitude and number of diodes activated between Mg^{2+}-free and Mg^{2+}-free + SAS, n = 6, $P < 0.001$. In addition, significant condition-by-stimulation intensity interactions between Mg^{2+}-free and Mg^{2+}-free + SAS means were also found. * = $P = 0.01$ ** = $P < 0.01$, *** = $P < 0.001$

we wanted to evaluate the efficacy of SAS on other models of hyperexcitability. To test this, $GABA_A$ receptor–mediated inhibition was blocked by the addition of bic to the perfusate, greatly enhancing the duration and lateral spread of the VSD signals, which is reflective of network hyperexcitability. In VSD recordings, application of SAS significantly decreased the peak amplitude (Figure 4A,B, $P < 0.001$) and spread (Figure 4A,B, $P < 0.001$) of bic-induced network hyperactivity. On the other hand, in whole-cell recordings, SAS did not change the number of epileptiform discharges (bic: 13.14 ± 7.67; SAS: 13.43 ± 7.52, $P = 0.85$, Figure 4C,D), but did significantly reduce the duration of the events (bic: 2.21 ± 1.86 seconds; SAS 0.82 ± 1.00 seconds, $P = 0.01$, Figure 4C,D). Next, we tested the effects of SAS on epileptiform activity induced by application of 4-AP, which blocks voltage-activated K^+ channels. In VSD recordings, 4-AP augmented the spatiotemporal spread of activity across the cortex. SAS significantly reduced the peak amplitude, indicated by the decrease in warmer colors (Figure 5A,B, $P < 0.001$), and responses were restricted to the vicinity of the stimulation (Figure 5A,B, $P < 0.001$). In whole-cell recordings, 4-AP induced events that were completely blocked by SAS (4-AP: 93 ± 66.62; SAS: 0.5 ± 0.84, $P = 0.02$, Figure 5C,D) at the end of the recording. The duration of the few remaining events

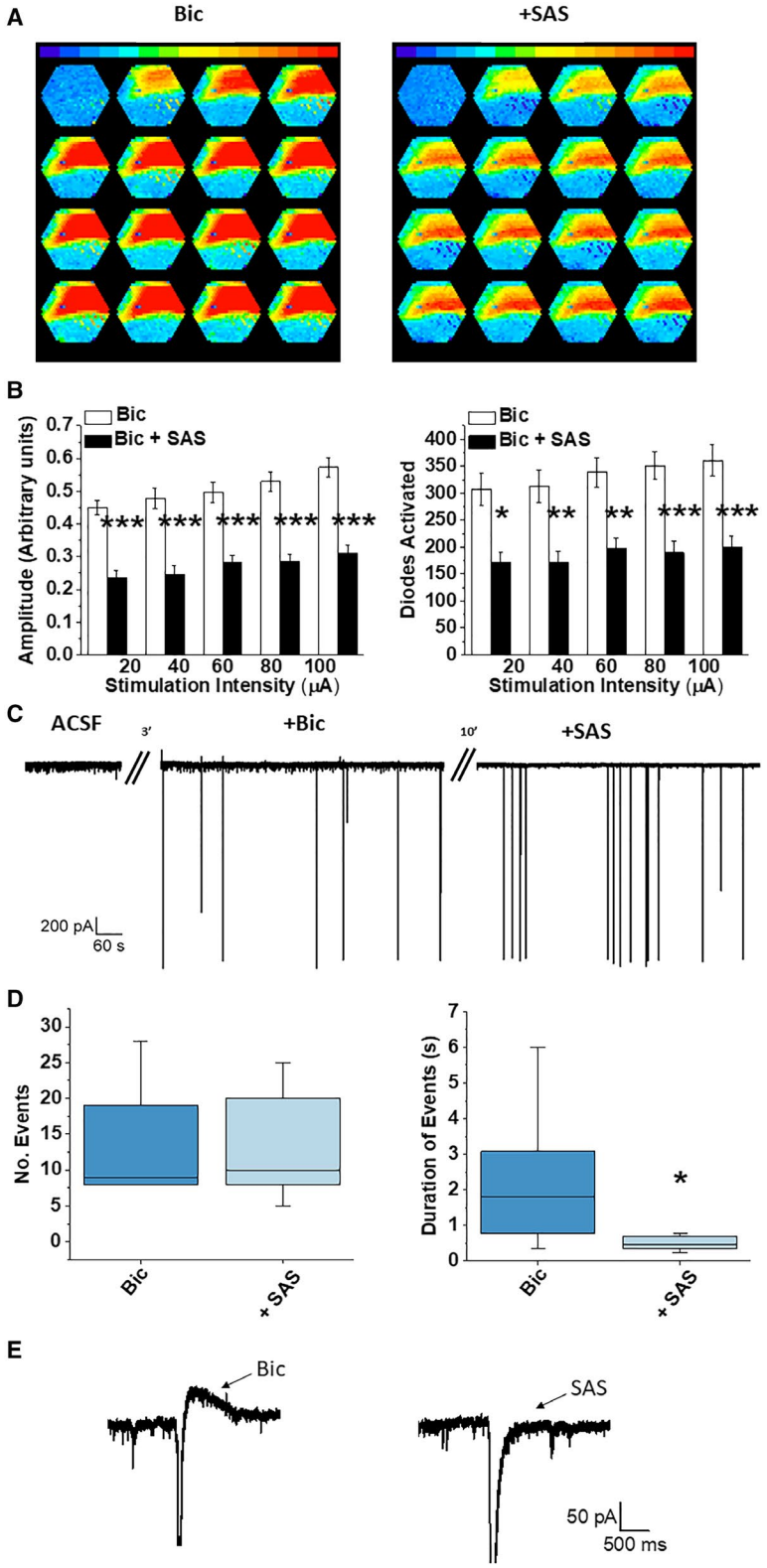

FIGURE 4 SAS decreases spatiotemporal spread of bic-induced network activity and epileptiform events. A, A pseudocolor map of the spatiotemporal patterns of activity evoked by intracortical stimulation in the presence of bic (left) and after application of SAS (right) at the same stimulation intensity. B, Quantitative summary of the amplitude and spread of bic-induced epileptiform activity using VSD recordings. Application of SAS significantly decreased the response amplitude and number of diodes activated between bic and bic + SAS, n = 6, $P < 0.001$. Significantly different condition-by-stimulation intensity interactions between bic and bic + SAS means were also found. * = $P = 0.01$ ** = $P < 0.01$, *** = $P < 0.001$. C, Representative traces of whole-cell patch clamp recordings in ACSF (left), bic (middle), and SAS (right). D, Quantitative summary of the number and duration of epileptiform events detected in whole-cell patch clamp recordings. * = significantly different from bic, n = 7, $P = 0.01$. E, Magnified bic (left) and SAS (right) traces during an epileptiform event

significantly decreased (4-AP: 2.16 ± 1.00 seconds; SAS: 0.14 ± 0.22 seconds, $P = 0.005$, Figure 5C,D) before being blocked at the end of the recording. Together these findings suggest that SAS can decrease the spread of epileptiform activity induced by different pharmacologic agents, with distinct mechanism of action.

3.6 | The effect of co-application of SAS and AEDs on cortical network activity

Because polypharmacy is used increasingly in the management of intractable epilepsy, we examined whether coapplication of a clinically approved AED and SAS would

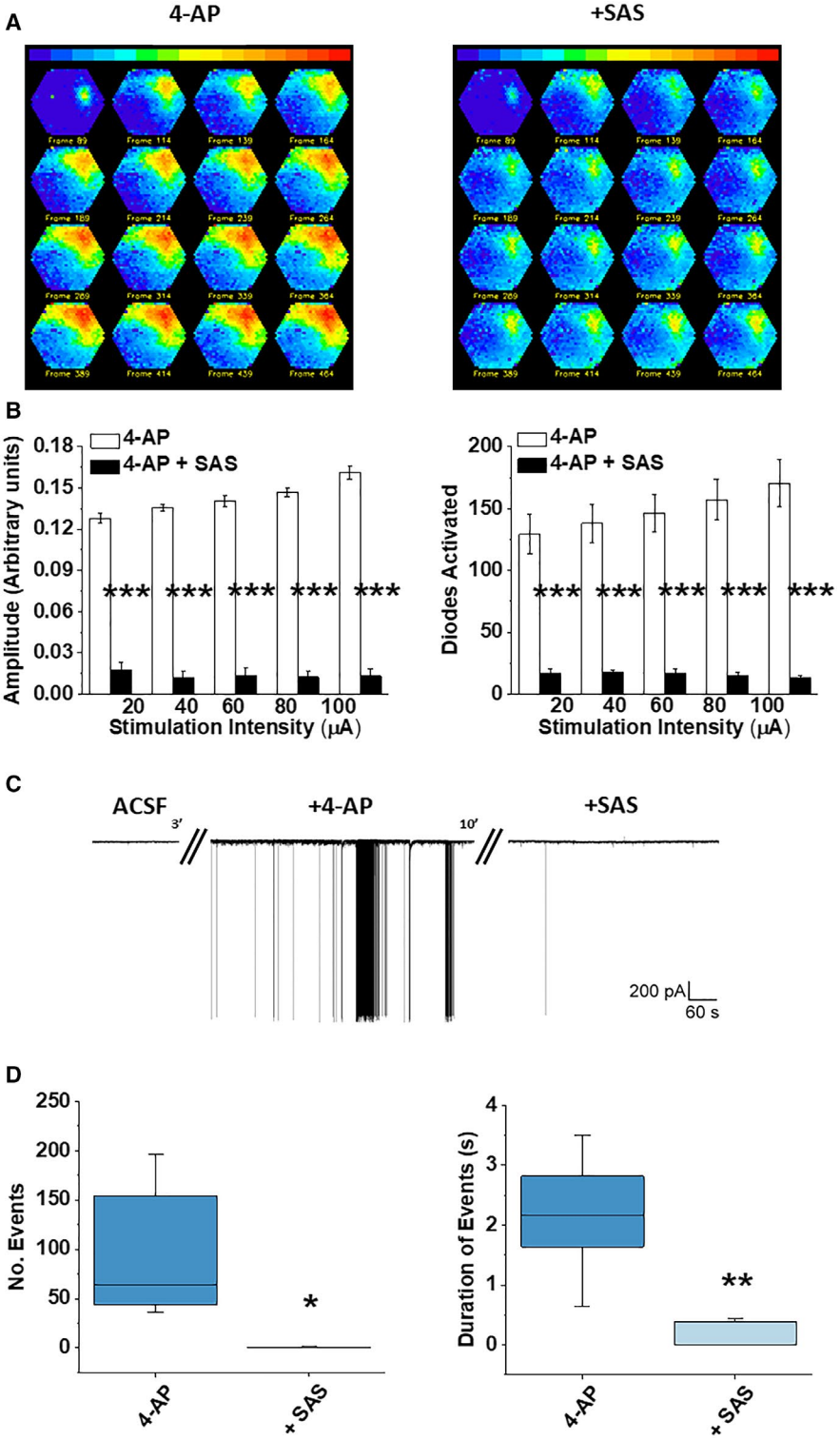

FIGURE 5 SAS blocks 4-AP–mediated epileptiform and VSD network response. A, Representative spatiotemporal patterns of activity evoked by a single pulse stimulation in the presence of 4-AP (left) and after application of SAS (right). SAS exhibits a net inhibitory effect on the activity evoked by 4-AP. B, Summary of the amplitude and spread of 4-AP–mediated epileptiform activity using VSD recordings. Application of SAS significantly decreased the response amplitude and number of diodes activated between 4-AP and 4-AP + SAS, n = 8, $P < 0.001$. Significant condition-by-stimulation intensity interactions between 4-AP and 4-AP + SAS means were also found. *** = $P < 0.001$. C, Specimen recording showing a complete block of ictal and interictal 4-AP–induced epileptiform activity (middle) upon application with SAS (right). D, Quantitative summary of the number and duration of epileptiform events detected in whole-cell patch clamp recordings. * = SAS application significantly different than 4-AP, $P = 0.02$ ** = SAS significantly different than 4-AP, $P = 0.005$. n = 6

result in synergistic antiepileptic effects compared to the AED alone. In VSD recordings, bath infusion of LEV to 4-AP–induced network activity (Figure 6A, left and middle) resulted in a significant decrease in peak amplitude (Figure 6A,B, $P < 0.001$) and spread (Figure 6A,B, $P < 0.001$) of network activity, yet co-application of SAS with LEV (Figure 6A, right) did not result in a significant change in amplitude peak (Figure 6A,B, $P > 0.05$) or spread (Figure 6A,B, $P > 0.05$) of network response. Similarly, when LEV was applied to Mg^{2+}-free–induced epileptiform activity (Figure 6C, left and middle) it significantly decreased the peak amplitude (Figure 6C,D, $P < 0.001$) and spread (Figure 6C,D, $P < 0.001$) of network activity. However, co-application of SAS with LEV in Mg^{2+}-free (Figure 6C, right) ACSF did not result in a significant change in peak amplitude (Figure 6C,D, $P > 0.05$) and

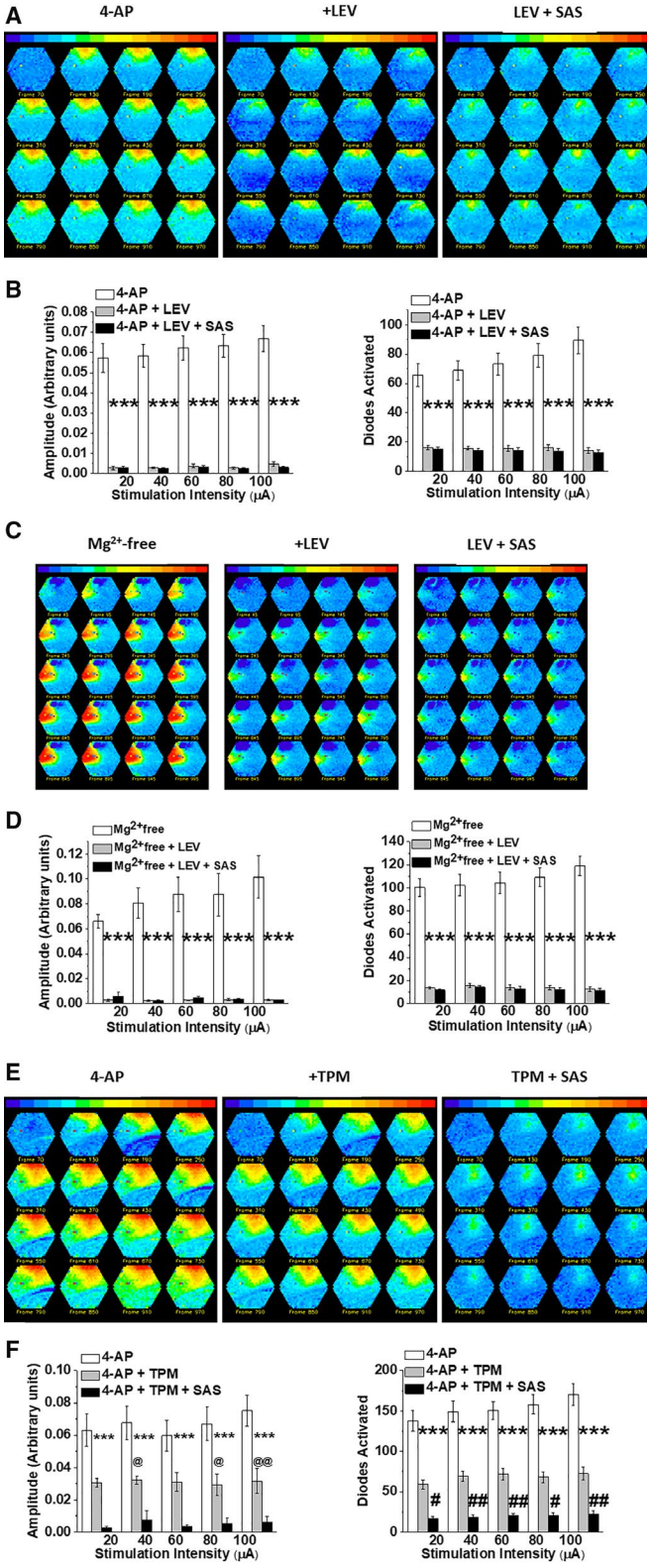

FIGURE 6 Comparison of VSD signals in response to co-application of AEDs and SAS. A, Spatiotemporal patterns of activity evoked in the upper cortical layers in 4-AP (left), after application of LEV (middle) and after co-application with SAS (right). B, Quantitative summary of the amplitude and spread of 4-AP–mediated VSD signal in the presence of LEV and LEV + SAS (n = 9). A significant decrease was found in the response amplitude and number of diodes activated between the different conditions (4-AP, 4-AP + LEV, 4-AP + LEV + SAS). $P < 0.001$. Significant condition-by-stimulation intensity interactions in the means of the response amplitude and number of diodes activated between 4-AP and 4-AP + LEV, and 4-AP and 4-AP + LEV + SAS, were also found. *** = $P < 0.001$. No significant difference was found between LEV and co-application of LEV + SAS. C, Network activity evoked in cortical layer II/III in Mg^{2+}-free ACSF (left), after application of LEV (middle) and following co-application of SAS (right). D, Summary bar graphs of the amplitude and spread of Mg^{2+}-free epileptiform activity in the presence of LEV and LEV + SAS (n = 9). A significant decrease in the response amplitude and number of diodes activated between the different conditions (Mg^{2+}-free, Mg^{2+}-free + LEV, Mg^{2+}-free + LEV + SAS). $P < 0.001$. Significant condition-by-stimulation intensity interactions in the means of the response amplitude and number of diodes activated between Mg^{2+}-free and Mg^{2+}-free + LEV, and Mg^{2+}-free and Mg^{2+}-free + LEV + SAS were also found. *** = $P < 0.001$. No significant difference was found between LEV and co-application of LEV + SAS. E, Spatiotemporal patterns of activity evoked in 4-AP (left), after application of TPM (middle) and after co-application of SAS (right). F, Summary bar graphs of the amplitude and spread of 4-AP–mediated epileptiform activity in the presence of TPM and TPM + SAS (n = 7). Significant decreases were found in the response amplitude and number of diodes activated between the different conditions (4-AP, 4-AP + TPM, 4-AP + TPM + SAS). $P < 0.001$. Significant condition-by-stimulation intensity interactions in the means of response amplitudes at stimulation intensities of 20, 80, and 100 μAs between 4-AP and 4-AP + TPM were also found. @ = $P < 0.05$, @@ = $P = 0.002$. Interactions in amplitude response between 4-AP and 4-AP + TPM + SAS were significant at all stimulation intensities, *** = $P < 0.001$. No significant interaction was found between 4-AP + TPM and 4-AP + TPM + SAS response amplitudes. Significant condition-by-stimulation intensity interactions were found in the number of diodes activated between 4-AP and 4-AP + TPM, and 4-AP and 4-AP + LEV + SAS, *** = $P < 0.001$. In addition, significant interactions between the number of diodes activated in 4-AP + TPM and 4-AP + TPM + SAS were found at all stimulation intensities, # = $P < 0.05$, ## = $P < 0.01$

spread (Figure 6C,D, $P > 0.05$) of neuronal network activity. We next examined the synergistic effects of SAS with another clinically approved AED, TPM. In the presence of 4-AP, application of TPM (Figure 6E, left and middle) decreased the peak amplitude (Figure 6E,F, $P < 0.001$) and spread (Figure 6E,F, $P < 0.001$) of VSD response. Co-application of SAS with TPM (Figure 6E, right) resulted in a vast additional reduction of peak amplitude (Figure 6E,F, $P < 0.05$) and spread (Figure 6E,F, $P < 0.05$) of 4-AP–induced VSD signal, compared to the effects of TPM alone. Altogether, our results indicate that SAS significantly reduces the spatiotemporal spread of cortical network activity in all three hyperexcitability models. In addition,

concomitant use of TPM and SAS resulted in additional antiepileptic effects compared to the use of TPM alone.

4 | DISCUSSION

Recent studies demonstrate that SAS is involved in modulating glutamate levels. We found that SAS modulates both evoked excitatory and inhibitory postsynaptic currents. We also show that SAS can decrease network hyperexcitability in three pharmacologically induced models. Furthermore, SAS is more efficacious in inhibiting 4-AP–induced network activity compared to the currently prescribed AED TPM.

We first used patch-clamp recordings to explore the effect of SAS on evoked EPSCs in layer II/III pyramidal neurons and observed that SAS (as well as S-4CPG) decreased EPSC amplitude via a reduction in NMDAR-mediated currents. These results support previous in vitro studies that sought to characterize the NMDA antagonistic properties of SAS.[16,17] Our results show that SAS decreased both the amplitude and frequency of sEPSCs, which suggests that it could be acting via both pre- and postsynaptic mechanisms. Surprisingly we found that although SAS decreased the amplitude of eIPSCs, it significantly prolonged the τ_{slow}. The increase in the τ_{slow} could have a significant inhibitory effect by prolonging inhibitory currents, but also questions the possible effect of SAS on GABA-uptake mechanisms. More studies are needed to better understand the effects of SAS on inhibition.

The objective of this study is to elucidate the global effects of SAS-mediated inhibition of SXC in distinct models of hyperexcitability, as a proxy for the hyperexcitable brain microenvironment in patients with epilepsy. We used acute cortical slices from C7Bl6 mice bathed in Mg^{2+}-free, bic or 4-AP–containing ACSF to simulate cortical network hyperexcitability. Under these conditions, we found that SAS significantly reduced the amplitude and spread of evoked epileptiform activity in all hyperexcitability models tested. Notably, we observed that in VSD recordings SAS reduced the optical response in both Mg^{2+}-free and bic-containing ACSF, but SAS did not reduce the number of epileptiform events in whole-cell patch-clamp recordings. Instead, SAS decreased the duration of the epileptiform events in all the models tested. The latter is similar to the effect of AEDs on 4-AP–-induced epileptiform activity, where ictal events but not interictal events were abolished.[20,21] As reported by D'Antuono et al (2010), epileptiform discharges induced by 4-AP in the entorhinal cortex were sensitive to carbamazepine and TPM, by blocking ictal events but not interictal. However, in our study, SAS surprisingly completely blocked all 4-AP–induced epileptiform activity in the prefrontal cortex. This was observed at the single cell level, where application of SAS first caused a decrease in the duration of epileptiform events and later completely blocked epileptiform events, and also at the network level by significantly decreasing VSD optical signals. In the presence of bic-induced epileptiform events, SAS decreased the spread of the VSD optical signal but not the number of epileptiform events in whole-cell recordings. During these experiments, we observed either an increase or no change in the number of events, but there was a consistent decrease in the duration of the events in all experiments. When hyperexcitability was induced by Mg^{2+}-free solution, the spread and duration of VSD optical signal was decreased. Under the same conditions, in whole-cell recordings, SAS significantly decreased the duration of epileptiform events and increased the number of events, supporting previous findings of blocking ictal but not interictal events.[10] Differential changes in the parameters of epileptiform activity have been described in the entorhinal cortex of kainate-treated rats in response to several AEDs.[22] The findings from these experiments validate the ability of SAS to decrease hyperexcitability induced by different mechanisms.

Based on the significant effect of SAS on 4-AP–induced epileptiform events, we questioned how it compares to currently prescribed AEDs. We found that LEV significantly decreased the spread and duration of both 4-AP- and Mg^{2+}-free-induced VSD optical signal and co-application of SAS did not significantly affect the small remaining VSD optical signal. However, we found that although TPM partially decreased the spread and duration of VSD optical signal induced by 4-AP, it was to a lesser degree compared to the inhibition by LEV. When SAS was later co-applied with TPM, it caused a significant decrease in the remaining VSD optical signal. It is worth noting that in the present study a single drug concentration of SAS and AEDs was chosen based on previous studies, and a more rigorous pharmacologic study would be necessary to fully compare the efficacy of SAS to AEDs.

Although it is estimated that one in 26 people develop epilepsy within their lifetime,[23] current AEDs are not effective for a third of affected patients.[24] This unmet need has led to the development of 17 clinically approved AEDs in the last 30 years.[25] The rise in the number of clinically available AEDs resulted in the use of polytherapy to address drug-resistant epilepsies. However, the efficacy of polytherapy has been debated as different studies have demonstrated mixed results.[26–28] One possible explanation for the limited efficacy of polytherapy in drug-resistant epilepsies may be due to current AEDs targeting primarily neuronal processes. As more evidence regarding the contributions of glial processes in epileptogenesis continues to become unveiled[29–32] the prospect of novel, nonneuronal targets involved in seizure generation and epileptogenesis is encouraging. Given that increased SXC expression has been found in human epileptic tissue[33] and the strong link between aberrant SXC expression in tumor-associated epilepsy, further studies on SXC as a target for acquired epilepsy are warranted. SXC's inhibition

by SAS provides a novel, nonneuronal treatment modality for decreasing release of excitatory glutamate in the brain.

Based on our findings, we propose that SAS inhibits SXC primarily on astrocytes to cause a decrease in ambient, extracellular glutamate concentrations, which results in decreased activity of extrasynaptic NMDARs, leading to suppression of slow-transient currents. Pharmacologic inhibition of SXC in rats reduces extracellular glutamate by 60%[34] and genetic knock-out of SXC in mice and drosophila results in a significant decrease in extracellular glutamate[8,35] More studies are required to determine specific changes on glutathione.

In conclusion, we demonstrate that SAS can decrease three pharmacologically induced models of cortical network hyperexcitability. Finally, SAS was more efficacious in decreasing the spread and duration of 4-AP–induced VSD optical response compared to the currently prescribed AED TPM, suggesting that it could be explored as a potential adjuvant treatment for seizures.

ACKNOWLEDGMENTS

This work was supported by US National Institutes of Health grants RO1-NS052634, 5RO1-NS036692, and R01CA227149, and start-up funds from the College of Agricultural and Life Sciences and the College of Science at Virginia Tech, United States. We thank Dr. John J. Hablitz at the University of Alabama at Birmingham for the use of his voltage-sensitive dye setup.

CONFLICT OF INTEREST

The authors have no conflict of interest to report. We confirm that we have read the Journal's position on issues involved in ethical publication and affirm that this report is consistent with those guidelines.

ORCID

Susan L. Campbell https://orcid.org/0000-0001-7775-8600

REFERENCES

1. Epilepsy: WHO; 2018[updated February 8, 2018. Available from: http://www.who.int/news-room/fact-sheets/detail/epilepsy.
2. Brodie MJ, Barry SJ, Bamagous GA, Norrie JD, Kwan P. Patterns of treatment response in newly diagnosed epilepsy. Neurology. 2012;78:1548–54.
3. Löscher W, Schmidt D. Modern antiepileptic drug development has failed to deliver: ways out of the current dilemma. Epilepsia. 2011;52:657–78.
4. Devinsky O, Vezzani A, Najjar S, De Lanerolle NC, Rogawski MA. Glia and epilepsy: excitability and inflammation. Trends Neurosci. 2013;36:174–84.
5. Coulter DA, Steinhäuser C. Role of astrocytes in epilepsy. Cold Spring Harb Perspect Med. 2015;5:a022434.
6. Binder DK. Astrocytes: stars of the Sacred Disease. Epilepsy Curr. 2018;18:172–9.
7. Massie A, Boillee S, Hewett S, Knackstedt L, Lewerenz J. Main path and byways: non-vesicular glutamate release by system xc(-) as an important modifier of glutamatergic neurotransmission. J Neurochem. 2015;135:1062–79.
8. De Bundel D, Schallier A, Loyens E, Fernando R, Miyashita H, Van Liefferinge J. Loss of system x(c)- does not induce oxidative stress but decreases extracellular glutamate in hippocampus and influences spatial working memory and limbic seizure susceptibility. J Neurosci. 2011;31:5792–803.
9. Bridges R, Lutgen V, Lobner D, Baker DA. Thinking outside the cleft to understand synaptic activity: contribution of the cystine-glutamate antiporter (System xc-) to normal and pathological glutamatergic signaling. Pharmacol Rev. 2012;64:780–802.
10. Buckingham SC, Campbell SL, Haas BR, Montana V, Robel S, Ogunrinu T, et al. Glutamate release by primary brain tumors induces epileptic activity. Nat Med. 2011;17:1269–U299.
11. Robert SM, Buckingham SC, Campbell SL, Robel S, Holt KT, Ogunrinu-Babarinde T, et al. SLC7A11 expression is associated with seizures and predicts poor survival in patients with malignant glioma. Sci Transl Med. 2015;7:289ra86.
12. Noebels JL, Avoli M, Rogawski M, Olsen R, Delgado-Escueta AV. Jasper's Basic Mechanisms of the Epilepsies Workshop. Epilepsia. 2010;51(Suppl 5):1–5.
13. Kampa BM, Clements J, Jonas P, Stuart GJ. Kinetics of Mg2 + unblock of NMDA receptors: implications for spike-timing dependent synaptic plasticity. J Physiol-London. 2004;556:337–45.
14. Glauser T, Ben-Menachem E, Bourgeois B, Cnaan A, Guerreiro C, Kälviäinen R, et al. Updated ILAE evidence review of antiepileptic drug efficacy and effectiveness as initial monotherapy for epileptic seizures and syndromes. Epilepsia. 2013;54:551–63.
15. DeFazio RA, Hablitz JJ. Horizontal spread of activity in neocortical inhibitory networks. Brain Res Dev Brain Res. 2005;157:83–92.
16. Ryu BR, Lee YA, Won SJ, Noh JH, Chang SY, Chung JM, et al. The novel neuroprotective action of sulfasalazine through blockade of NMDA receptors. J Pharmacol Exp Ther. 2003;305:48–56.
17. Noh JH, Gwag BJ, Chung JM. Underlying mechanism for NMDA receptor antagonism by the anti-inflammatory drug, sulfasalazine, in mouse cortical neurons. Neuropharmacology. 2006;50:1–15.
18. Yuste R, Tank DW, Kleinfeld D. Functional study of the rat cortical microcircuitry with voltage-sensitive dye imaging of neocortical slices. Cereb Cortex. 1997;7:546–58.
19. Langenstroth M, Albowitz B, Kuhnt U. Partial suppression of GABAA-mediated inhibition induces spatially restricted epileptiform activity in guinea pig neocortical slices. Neurosci Lett. 1996;210:103–6.
20. D'Antuono M, Köhling R, Ricalzone S, Gotman J, Biagini G, Avoli M. Antiepileptic drugs abolish ictal but not interictal epileptiform discharges in vitro. Epilepsia. 2010;51:423–31.
21. Gotman J, Marciani MG. Electroencephalographic spiking activity, drug levels, and seizure occurrence in epileptic patients. Ann Neurol. 1985;17:597–603.
22. West PJ, Saunders GW, Billingsley P, Smith MD, White HS, Metcalf CS, et al. Recurrent epileptiform discharges in the medial entorhinal cortex of kainate-treated rats are differentially sensitive to antiseizure drugs. Epilepsia. 2018;59:2035–48.

23. Hesdorffer DC, Logroscino G, Benn EK, Katri N, Cascino G, Hauser WA. Estimating risk for developing epilepsy: a population-based study in Rochester, Minnesota. Neurology. 2011;76:23–7.
24. Kwan P, Schachter SC, Brodie MJ. Drug-resistant epilepsy. N Engl J Med. 2011;365:919–26.
25. Campos G, Fortuna A, Falcão A, Alves G. In vitro and in vivo experimental models employed in the discovery and development of antiepileptic drugs for pharmacoresistant epilepsy. Epilepsy Res. 2018;146:63–86.
26. Brodie MJ, Yuen AW. Lamotrigine substitution study: evidence for synergism with sodium valproate? 105 Study Group. Epilepsy Res. 1997;26:423–32.
27. Pisani F, Oteri G, Russo MF, Di Perri R, Perucca E, Richens A. The efficacy of valproate-lamotrigine comedication in refractory complex partial seizures: evidence for a pharmacodynamic interaction. Epilepsia. 1999;40:1141–6.
28. Beyenburg S, Stavem K, Schmidt D. Placebo-corrected efficacy of modern antiepileptic drugs for refractory epilepsy: systematic review and meta-analysis. Epilepsia. 2010;51:7–26.
29. Vargas-Sánchez K, Mogilevskaya M, Rodríguez-Pérez J, Rubiano MG, Javela JJ, González-Reyes RE. Astroglial role in the pathophysiology of status. Oncotarget. 2018;9:26954–76.
30. Eid T, Lee TW, Patrylo P, Zaveri HP. Astrocytes and Glutamine Synthetase in Epileptogenesis. J Neurosci Res. 2018. [Epub ahead of print].
31. Boison D, Steinhäuser C. Epilepsy and astrocyte energy metabolism. Glia. 2018;66:1235–43.
32. Binder DK, Steinhäuser C. Functional changes in astroglial cells in epilepsy. Glia. 2006;54:358–68.
33. Lewerenz J, Baxter P, Kassubek R, Albrecht P, Van Liefferinge J, Westhoff MA, et al. Phosphoinositide 3-kinases upregulate system xc(-) via eukaryotic initiation factor 2α and activating transcription factor 4 - A pathway active in glioblastomas and epilepsy. Antioxid Redox Signal. 2014;20:2907–22.
34. Baker DA, Xi ZX, Shen H, Swanson CJ, Kalivas PW. The origin and neuronal function of in vivo nonsynaptic glutamate. J Neurosci. 2002;22:9134–41.
35. Augustin H, Grosjean Y, Chen K, Sheng Q, Featherstone DE. Nonvesicular release of glutamate by glial xCT transporters suppresses glutamate receptor clustering in vivo. J Neurosci. 2007;27:111–23.

How to cite this article: Alcoreza O, Tewari BP, Bouslog A, Savoia A, Sontheimer H, Campbell SL. Sulfasalazine decreases mouse cortical hyperexcitability. *Epilepsia*. 2019;60:1365–1377. https://doi.org/10.1111/epi.16073